

## Superconductivity in New Iron Pnictide Oxide (Fe<sub>2</sub>As<sub>2</sub>)(Sr<sub>4</sub>(Mg,Ti)<sub>2</sub>O<sub>6</sub>)

Shinya Sato<sup>1,4</sup>, Hiraku Ogino<sup>1,4\*</sup>, Naoto Kawaguchi<sup>1,4</sup>, Yukari Katsura<sup>2</sup>, Kohji Kishio<sup>1,4</sup>, Jun-ichi Shimoyama<sup>1,4</sup>, Hisashi Kotegawa<sup>3,4</sup> and Hideki Tou<sup>3,4</sup>

<sup>1</sup>Department of Applied Chemistry, The University of Tokyo, 7-3-1 Hongo, Bunkyo-ku, Tokyo 113-8656, Japan

<sup>2</sup>Magnetic Materials Laboratory, RIKEN, 2-1 Hirosawa, Wako-shi, Saitama 351-0106 Japan

<sup>3</sup>Department of Physics, Kobe University, Kobe 657-8501

<sup>4</sup>JST-TRIP, Sanban-cho, Chiyoda-ku, Tokyo 102-0075, Japan

e-mail address : tuogino@mail.ecc.u-tokyo.ac.jp

### Abstract

We have discovered a new iron pnictide oxide superconductor (Fe<sub>2</sub>As<sub>2</sub>)(Sr<sub>4</sub>(Mg,Ti)<sub>2</sub>O<sub>6</sub>). This material is isostructural with (Fe<sub>2</sub>As<sub>2</sub>)(Sr<sub>4</sub>M<sub>2</sub>O<sub>6</sub>) (*M* = Sc, Cr, V), which were found in previous studies. The structure of this compound is tetragonal with a space group of *P4/nmm* and consists of the anti-fluorite type FeAs layer and perovskite-type block layer. The lattice constants are *a* = 3.935 Å and *c* = 15.952 Å for (Fe<sub>2</sub>As<sub>2</sub>)(Sr<sub>4</sub>MgTiO<sub>6</sub>). Bulk superconductivity with *T*<sub>c(onset)</sub> of ~26 K was observed for a partially Co substituted sample. Moreover, Co-free and Ti-rich samples exhibited higher *T*<sub>c(onset)</sub>'s above 35 K, which were further enhanced by applying high pressures up to ~43 K.

**PACS** : 61.05.cp X-ray diffraction, 61.66.Fn Inorganic compounds, 74.70.-b Superconducting materials

**Keyword** : pnictide oxides, superconductor, perovskite structure

### Introduction

The discovery of high-*T*<sub>c</sub> superconductivity in LaFeAs(O,F)[1] has triggered researches for development of new iron pnictide superconductors. Until now, several groups of superconductors containing anti-fluorite pnictide or chalcogenide layer have been discovered such as REFeAsO (*RE* = rare earth elements) (abbreviated as 1111)[2],

$A\text{EFe}_2\text{As}_2$  ( $A\text{E}$  = alkali earth metals)[3],  $\text{LiFeAs}$ [4], and  $\text{FeSe}$ [5]. In addition, many layered compounds composed of both antiferromagnetic pnictide layer and perovskite-type oxide layer, such as  $(\text{Fe}_2\text{As}_2)(\text{Sr}_3\text{Sc}_2\text{O}_5)$ [6] and  $(\text{Fe}_2\text{P}_2)(\text{Sr}_4\text{Sc}_2\text{O}_6)$ [7], have been successively found.  $(\text{Fe}_2\text{P}_2)(\text{Sr}_4\text{Sc}_2\text{O}_6)$  having  $\text{K}_2\text{NiF}_4$ -type perovskite-related oxide layer showed superconductivity at 17 K, which is the highest value among the iron phosphide compounds. Its arsenic relatives  $(\text{Fe}_2\text{As}_2)(\text{Sr}_4M_2\text{O}_6)$  were also discovered in  $M = \text{Sc}, \text{Cr}$ [8,9] and  $\text{V}$ [10]. Large amount of Ti substitution for  $(\text{Fe}_2\text{As}_2)(\text{Sr}_4\text{Sc}_2\text{O}_6)$  and  $(\text{Fe}_2\text{As}_2)(\text{Sr}_4\text{Cr}_2\text{O}_6)$  were also suggested to be effective for inducing superconductivity[11,12]. Moreover,  $(\text{Fe}_2\text{As}_2)(\text{Sr}_4\text{V}_2\text{O}_6)$  was found to show superconductivity with  $T_{\text{c}(\text{onset})}$  of  $\sim 40$  K without intensive carrier doping[10,13] and  $T_{\text{c}(\text{onset})}$  increased up to 46 K under a pressure of 4 GPa[14]. These facts indicated that this system is a new vein of iron pnictide superconductors.

There are several perovskite oxides called “double perovskite”, which have mixed and ordered B-site cations, such as  $\text{LaMg}_{0.5}\text{Ti}_{0.5}\text{O}_3$ [15] and  $\text{LaZn}_{0.5}\text{Ti}_{0.5}\text{O}_3$ [16]. Since the  $\text{Sr}_4M_2\text{O}_6$  layer in above layered pnictide oxides have perovskite-type structure, where the  $M$ -site corresponds to the B-site of perovskite, mixing  $M$  elements was attempted to develop new layered oxide pnictide compounds in the present study. As a result, new iron arsenide oxide  $(\text{Fe}_2\text{As}_2)(\text{Sr}_4\text{MgTiO}_6)$  was successfully synthesized. Partial substitution of Co for the Fe-site was found to improve electronic state of this compound, resulting in bulk superconductivity with  $T_{\text{c}(\text{onset})}$  up to 26 K. This phase was also formed from Co-free and Ti-rich composition as a main phase. The superconducting properties of Co-free and Ti-rich compounds varied with the starting composition and the superconducting transition was observed up to 39 K.

## Experimental

All samples were synthesized by the solid-state reaction method starting from  $\text{FeAs}$ (3N),  $\text{CoAs}$ (3N),  $\text{SrO}$ (2N),  $\text{MgO}$ (3N),  $\text{Ti}$ (3N) and  $\text{TiO}_2$ (3N). Nominal compositions were fixed according to the general formula:  $(\text{Fe}_{1-x}\text{Co}_x)_2\text{As}_2(\text{Sr}_4(\text{Mg}_{1-y}\text{Ti}_y)_2\text{O}_6)$ . Since the starting reagent,  $\text{SrO}$ , is sensitive to moisture in air, manipulations were carried out under argon atmosphere. Powder mixture of  $\text{FeAs}$ ,  $\text{SrO}$ ,  $\text{MgO}$ ,  $\text{Ti}$  and  $\text{TiO}_2$  was pelletized and sealed in evacuated quartz ampoules. Heat-treatments were performed in the temperature range from 1000 to 1250°C for 40 to 72 hours. Phase identification was carried out by X-ray diffraction (XRD) using RIGAKU Ultima-IV diffractometer and intensity data were collected in the  $2\theta$  range of  $5^\circ - 80^\circ$  at a step of  $0.02^\circ$  using  $\text{Cu-K}\alpha$  radiation. Silicon powder was

used as the internal standard. High-resolution images were taken by a field-emission-type transmission electron microscopy (TEM, JEOL JEM-2010F). Magnetic susceptibility measurement was performed by a SQUID magnetometer (Quantum Design MPMS-XL5s). Electric resistivity was measured by the AC four-point-probe method under fields up to 9 T using Quantum Design PPMS. Electrical resistivity under high pressures was also measured using an indenter cell and Daphne 7474 as a pressure-transmitting medium[17,18]. Applied pressure was estimated from the  $T_c$  of the lead manometer.

## Result and discussion

Figure 1 shows a powder XRD pattern of  $(\text{Fe}_2\text{As}_2)(\text{Sr}_4\text{MgTiO}_6)$  reacted at 1200°C for 40 h together with a simulation pattern.  $(\text{Fe}_2\text{As}_2)(\text{Sr}_4\text{MgTiO}_6)$  was obtained as the main phase with a small amount of impurities, such as  $\text{SrFe}_2\text{As}_2$  and  $\text{FeAs}$ . Although several perovskite oxides with mixed B-site cation is known to have ordered structure accompanying orthorhombic distortion, the XRD pattern of  $(\text{Fe}_2\text{As}_2)(\text{Sr}_4\text{MgTiO}_6)$  could be indexed as space group of  $P4/nmm$  and lattice constants were determined to be  $a = 3.935 \text{ \AA}$  and  $c = 15.952 \text{ \AA}$ . The  $a$ -axis length was close to that of  $(\text{Fe}_2\text{As}_2)(\text{Sr}_4\text{V}_2\text{O}_6)$  with  $a = 3.930 \text{ \AA}$  and  $c = 15.666 \text{ \AA}$ [10], while the  $c$ -axis length is slightly longer.

Figure 2 shows a bright-field TEM image and an electron diffraction pattern taken from  $[1 -1 0]$  direction of a  $(\text{Fe}_2\text{As}_2)(\text{Sr}_4\text{MgTiO}_6)$  crystal. Both TEM image and electron diffraction patterns indicated tetragonal cell with  $c/a \sim 4.0$ , which coincided well with a corresponding value analyzed from XRD data. Any satellite spots suggesting superstructure due to ordering of B-site cations were not observed in the electron diffraction patterns.

Powder XRD patterns and lattice constants of  $((\text{Fe}_{1-x}\text{Co}_x)_2\text{As}_2)(\text{Sr}_4\text{MgTiO}_6)$  for  $0 \leq x \leq 0.15$  are shown in Fig. 3. Peak intensities of impurity phases did not increase by partial Co-substitution. The  $c$ -axis length systematically decreased with an increase in Co-substitution level,  $x$ , while the  $a$ -axis lengths were almost unchanged.

Temperature dependences of ZFC and FC magnetization for  $((\text{Fe}_{1-x}\text{Co}_x)_2\text{As}_2)(\text{Sr}_4\text{MgTiO}_6)$  with  $0 \leq x \leq 0.15$  measured under 1 Oe are shown in Fig. 4. The Co-free sample showed diamagnetism due to superconductivity with  $T_{c(\text{onset})}$  below 10 K and its volume fraction was only 1.5 %. On the other hand, large diamagnetism were observed in the Co-doped samples, and  $T_{c(\text{onset})}$  were 22 K, 24 K, 16 K for  $x = 0.05$ , 0.1 and 0.15, respectively. Figure 5 shows temperature dependence of resistivity for  $((\text{Fe}_{1-x}\text{Co}_x)_2\text{As}_2)(\text{Sr}_4\text{MgTiO}_6)$  with  $0 \leq x \leq 0.15$ . The metallic behaviors were observed in

the normal state resistivity for all samples and  $T_{c(\text{onset})}$  were  $\sim 10$  K,  $\sim 26$  K,  $\sim 26$  K and 18 K for  $x = 0, 0.05, 0.1$  and  $0.15$ , respectively. Zero resistivity was confirmed at 2 K, 15 K, 11 K and 9 K for  $x = 0, 0.05, 0.1$  and  $0.15$ , respectively. It should be noted that this is the first example of positive Co-substitution effect on superconducting properties of the  $(\text{Fe}_2\text{As}_2)(\text{Sr}_4\text{M}_2\text{O}_6)$  system.

Figure 6 shows powder XRD patterns of  $(\text{Fe}_2\text{As}_2)(\text{Sr}_4(\text{Mg}_{1-y}\text{Ti}_y)_2\text{O}_6)$  reacted at  $1200^\circ\text{C}$  for 40 h.  $(\text{Fe}_2\text{As}_2)(\text{Sr}_4(\text{Mg}_{1-y}\text{Ti}_y)_2\text{O}_6)$  phase was obtained for  $0.5 \leq y \leq 0.7$  as main phase, while peaks due to  $\text{SrFe}_2\text{As}_2$ ,  $\text{SrTiO}_3$  and other minor impurities increased with increasing  $y$ . On the other hand, Mg-rich compound was not formed judging from the abrupt increase in peak intensities of impurities and small changes in lattice constants. Any pnictide oxide phase could not be found in  $y = 1.0$ . For samples with  $0.5 \leq y \leq 0.7$ , the  $c$ -axis length systematically decreased with an increase of  $y$ , while it was difficult to calculate lattice constant for  $y = 0.8$  due to overlapping of diffraction peaks with impurities. This indicates that the compositional range of solid-solution exists towards Ti-rich composition.

Figure 7 shows backscattered electron images of a sample with a nominal composition of  $(\text{Fe}_2\text{As}_2)(\text{Sr}_4(\text{Mg}_{0.3}\text{Ti}_{0.7})_2\text{O}_6)$ . Three different grains were observed and EDX spectrum for each grains suggested that white, gray and black grains corresponded to  $\text{SrFe}_2\text{As}_2$ ,  $(\text{Fe}_2\text{As}_2)(\text{Sr}_4(\text{Mg},\text{Ti})_2\text{O}_6)$ , and  $\text{SrTiO}_3$  or  $\text{Sr}_2\text{TiO}_4$ , respectively.

Temperature dependences of ZFC and FC magnetization for  $(\text{Fe}_2\text{As}_2)(\text{Sr}_4(\text{Mg}_{1-y}\text{Ti}_y)_2\text{O}_6)$  of  $0.5 \leq y \leq 1$  measured under 1 Oe are shown in Fig. 8.  $T_{c(\text{onset})}$  increased with an increase of  $y$  up to 0.8, while superconducting volume fractions indicated by ZFC magnetization at low temperatures were large for samples with  $x = 0.6$  and  $0.7$ . In particular, samples with  $y = 0.55, 0.6$  and  $0.7$  exhibited large diamagnetism suggesting bulk superconductivity. The highest  $T_{c(\text{onset})}$  37 K was achieved by  $(\text{Fe}_2\text{As}_2)(\text{Sr}_4(\text{Mg}_{1-y}\text{Ti}_y)_2\text{O}_6)$  with  $y = 0.8$ . It should be noted that we confirmed that  $\text{SrFe}_2\text{As}_2$  did not show superconductivity even by doping of Ti, Mg or co-dopings of Ti and O or Mg and O.

Figure 9 shows temperature dependence of resistivity for  $(\text{Fe}_2\text{As}_2)(\text{Sr}_4(\text{Mg}_{1-y}\text{Ti}_y)_2\text{O}_6)$  of  $0.5 \leq y \leq 0.8$ . The metallic behaviors were observed in the normal state resistivity for all samples, and  $T_{c(\text{onset})}$  was  $\sim 33$  K,  $\sim 34$  K,  $\sim 36$  K and 39 K for  $y = 0.55, 0.6, 0.7$  and  $0.8$ , respectively. Zero resistivity was achieved at 14 K, 18 K, 22 K and 17 K for  $y = 0.55, 0.6, 0.7$  and  $0.8$ , respectively. These broad superconducting transitions indicate poor grain connectivity of the samples or inhomogeneous cation compositions.

The  $T_c$  increased systematically with an increase of  $y$  up to 39 K. In addition, superconducting volume fraction also increased with increasing  $y$ . Superconductivity in

Co-doped and Ti-rich samples indicates that electron doping is also effective in this compound as in the 1111 system. Very small superconducting volume fraction of the  $y = 0.5$  sample indicates that this compounds doesn't exhibit superconductivity intrinsically without intensive doping.

Figure 10 shows temperature dependence of resistances measured under various pressures for  $(\text{Fe}_2\text{As}_2)(\text{Sr}_4(\text{Mg}_{0.3}\text{Ti}_{0.7})_2\text{O}_6)$ . The  $T_{c(\text{onset})}$  increases with an increase of the pressure similarly in the case of  $(\text{Fe}_2\text{As}_2)(\text{Sr}_4\text{V}_2\text{O}_6)$ [14] and reaches  $\sim 43$  K at 4.2 GPa. The  $T_{c(\text{onset})}$  first increases largely by applied pressure with  $dT_c/dP = 2.5$  K/GPa and it seems to saturate at approximately 4 GPa.

## Conclusions

A new layered iron pnictide oxide  $((\text{Fe}_{1-x}\text{Co}_x)_2\text{As}_2)(\text{Sr}_4(\text{Mg}_{1-y}\text{Ti}_y)_2\text{O}_6)$  was synthesized and its physical properties were characterized. This material has alternate stacking of anti-fluorite  $\text{Fe}_2\text{As}_2$  and perovskite-type  $\text{Sr}_4(\text{Mg},\text{Ti})_2\text{O}_6$  layers. This compound exhibits superconductivity by partial substitution of Co for the Fe-site, and  $T_{c(\text{onset})}$  is 26 K at  $x = 0.05$ . This phase is also obtained as a main phase in the Ti-rich starting composition. In resistivity measurements, superconducting transition is observed up to 39 K under the ambient pressure, and it was increased up to  $\sim 43$  K by applying a high pressure of 4.2 GPa. These facts indicate that superconductivity of this compound is induced by the carrier control of the  $\text{Fe}_2\text{As}_2$  layer.

## Acknowledgement

This work was partly supported by Grant-in-Aid for Young Scientists (B) no. 21750187, 2009, supported by the Ministry of Education, Culture, Science and Technology (MEXT) as well as inter-university Cooperative Research Program of the Institute for Materials Research, Tohoku University.

## Figure captions

Figure 1. Powder XRD and simulation patterns of  $(\text{Fe}_2\text{As}_2)(\text{Sr}_4\text{MgTiO}_6)$ .

Figure 2. Bright-field TEM image and corresponding electron diffraction pattern of a  $(\text{Fe}_2\text{As}_2)(\text{Sr}_4\text{MgTiO}_6)$  crystal viewed from  $[1 -1 0]$  direction.

Figure 3. Powder XRD patterns and lattice constants of  $((\text{Fe}_{1-x}\text{Co}_x)\text{As}_2)(\text{Sr}_4\text{MgTiO}_6)$  for  $0 \leq x \leq 0.15$ .

Figure 4. Temperature dependence of ZFC and FC magnetization curves of  $((\text{Fe}_{1-x}\text{Co}_x)\text{As}_2)(\text{Sr}_4\text{MgTiO}_6)$  bulk samples measured under 1 Oe. Close-up of magnetization curves for  $((\text{Fe}_{1-x}\text{Co}_x)\text{As}_2)(\text{Sr}_4\text{MgTiO}_6)$  is shown in the inset.

Figure 5. Temperature dependences of resistivity for the  $((\text{Fe}_{1-x}\text{Co}_x)\text{As}_2)(\text{Sr}_4\text{MgTiO}_6)$  bulks at  $0 < T < 50$  K. Temperature dependences of resistivity at  $0 < T < 300$  K is shown in the inset.

Figure 6. Powder XRD patterns and lattice constants of  $(\text{Fe}_2\text{As}_2)(\text{Sr}_4(\text{Mg}_{1-y}\text{Ti}_y)_2\text{O}_6)$  for  $0.4 \leq y \leq 1$ .

Figure 7. Backscattered electron image of  $(\text{Fe}_2\text{As}_2)(\text{Sr}_4(\text{Mg}_{0.3}\text{Ti}_{0.7})_2\text{O}_6)$ .

Figure 8. Temperature dependence of ZFC and FC magnetization curves of  $(\text{Fe}_2\text{As}_2)(\text{Sr}_4(\text{Mg}_{1-y}\text{Ti}_y)_2\text{O}_6)$  bulk samples measured under 1 Oe. Close-up of the curves are shown in the inset.

Figure 9. Temperature dependences of resistivity for the  $(\text{Fe}_2\text{As}_2)(\text{Sr}_4(\text{Mg}_{1-y}\text{Ti}_y)_2\text{O}_6)$  bulks at  $0 < T < 50$  K. Temperature dependences of resistivity at  $0 < T < 300$  K is shown in the inset.

Figure 10. Temperature dependences of resistance under various pressure for the  $(\text{Fe}_2\text{As}_2)(\text{Sr}_4(\text{Mg}_{0.3}\text{Ti}_{0.7})_2\text{O}_6)$  bulks at  $20 < T < 60$  K. Temperature dependences of resistivity at  $0 < T < 300$  K is shown in the inset.

## References

- [1] Kamihara Y, Watanabe T, Hirano M and Hosono H, 2008 *J. Am. Chem. Soc.* **130** 3296.
- [2] Quebe P, Terbüchte L, W. Jeitschko W, 2000 *J. Alloys Compd.* **302** 70.
- [3] Rotter M, Tegel M and Johrendt D, 2008 *Phys. Rev. Lett.* **101** 107006.
- [4] Pitcher M, Parker D, Adamson P, Herkelrath S, Boothroyd A, Ibberson R, Brunelli M and Clarke S, 2008 *Chem. Commun.* **45** 5918

- [5] Hsu F.C, Luo J.Y, The K.W, Chen T.K, Huang T.W, Wu P.M, Lee Y.C, Huang Y.L, Chu Y.Y, Yan D.C and Wu M.K, 2008 *Proc. Natl. Acad. Sci. U.S.A.* **105** 14262..
- [6] Zhu X, Han F, Mu G, Zeng B, Cheng P, Shen B, Wen H-H, 2009 *Phys. Rev. B* **79** 024516.
- [7] Ogino H, Matsumura Y, Katsura Y, Ushiyama K, Horii S, Kishio K and Shimoyama J. 2009 *Supercond. Sci. Technol.* **22** 075008.
- [8] Ogino H, Katsura Y, Horii S, Kishio K and Shimoyama J, 2009 *Supercond. Sci. Technol.* **22** 085001.
- [9] Tegel M, Hummel F, Lackner S, Schellenberg I, Pöttgen R, and Johrendt D, 2009 arXiv : Condmat / 0904.0479(unpublished).
- [10] Zhu X, Han F, Mu G, Cheng P, Shen B, Zeng B and Wen H-H, 2009 *Phys. Rev. B* **79** 220512(R).
- [11] Chen G.F, Xia T.L, Yang H.X, Li J.Q, Zheng P, Luo J.L and Wang N.L, 2009 *Supercond. Sci. Technol.* **22** 072001.
- [12] Zhu X, Han F, Mu G, Cheng P, Shen B, Zeng B and Wen H-H, 2009 arXiv : Condmat / 0904. 0972.
- [13] Han F, Zhu X, Mu G, Cheng P, Shen B, Zeng B and Wen H-H, 2009 arXiv : Condmat / 0910. 1537.
- [14] Kotegawa H, Kawazoe T, Tou H, Murata K, Ogino H, Kishio K, Shimoyama, 2009 arXiv : Condmat / 0908. 1469(unpublished).
- [15] Lee D.Y, Yoon S-J, Yeo J.H, Nahm S, Paik J.H, Whang K-C and Ahn B.G, 2000 *J. Mater. Sci. Lett.* **19** 131-134
- [16] Ubc R, Hu Y and Abrahams I, 2006 *Acta Crystallogr. B* **62** 521-529.
- [17] Kobayashi T.C, Hidaka H, Kotegawa H, Fujiwara K, and Eremets M.I, 2007 *Rev. Sci. Instrum.* **78** 023909.
- [18] Murata K, Yokogawa K, Yoshino H, Klotz S, Munsch P, Irizawa A, Nishiyama M, Iizuka K, Nanba T, Okada T, Shiraga Y, and Aoyama S, 2008 *Rev. Sci. Instrum.* **79** 085101.

Figure 1

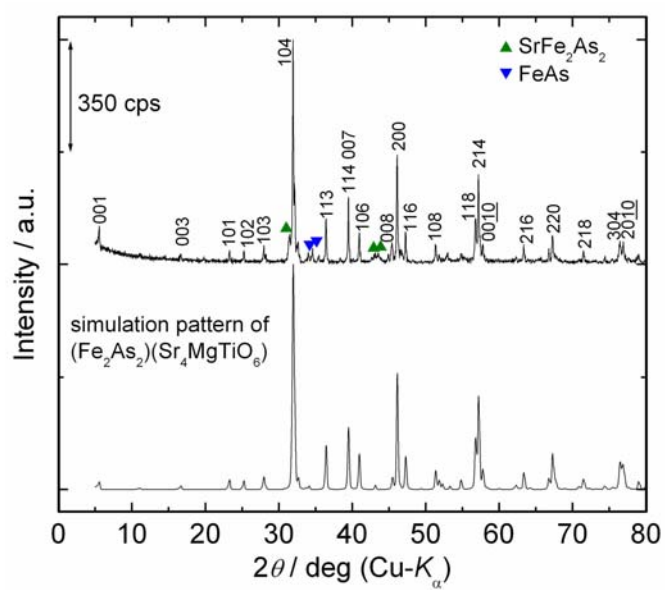


Figure 2

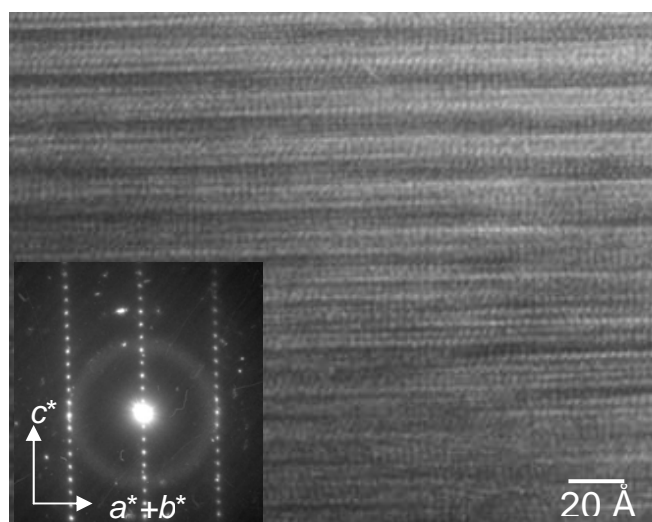




Figure 3

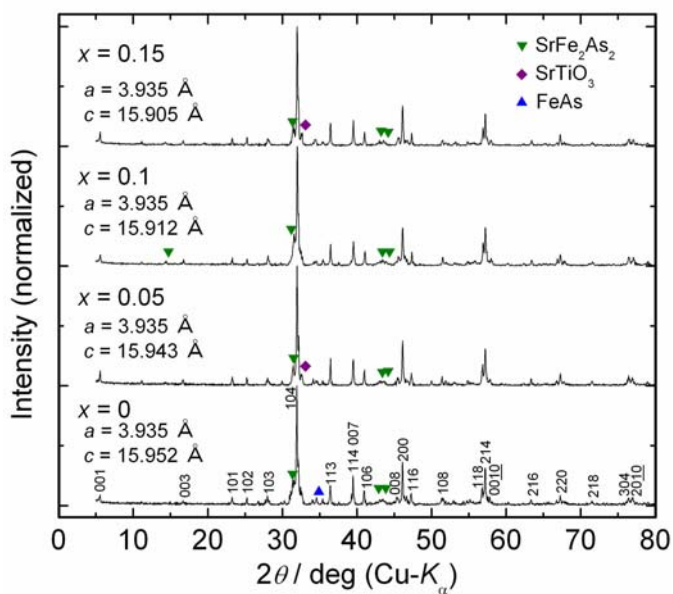


Figure 4

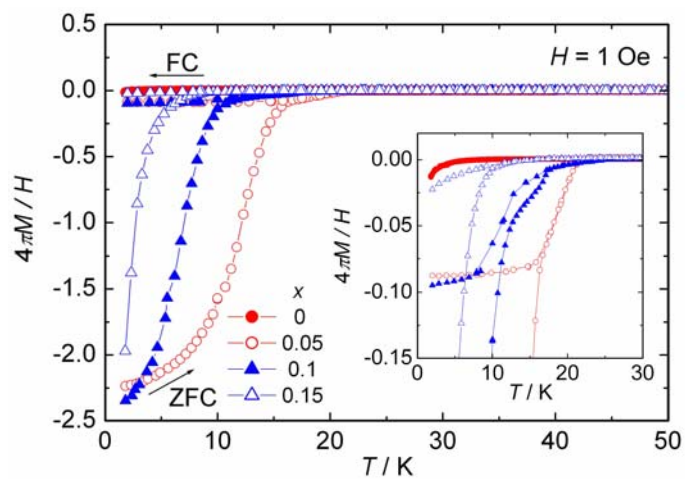


Figure 5

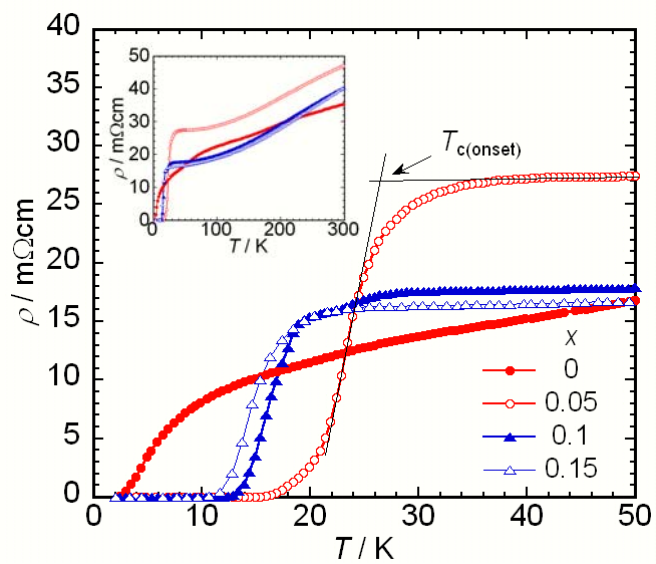


Figure 6

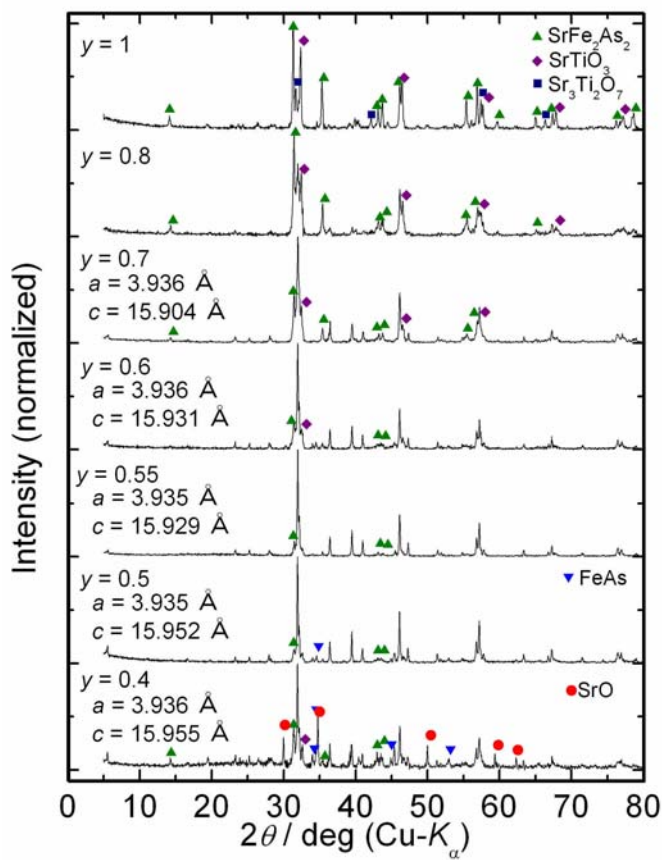


Figure 7

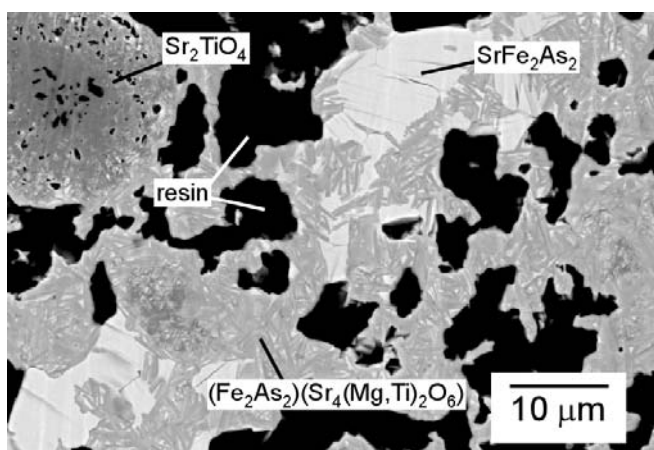


Figure 8

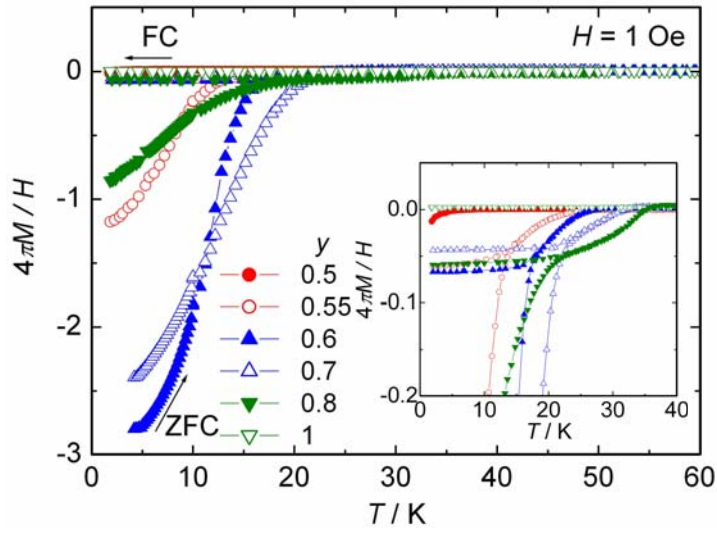


Figure 9

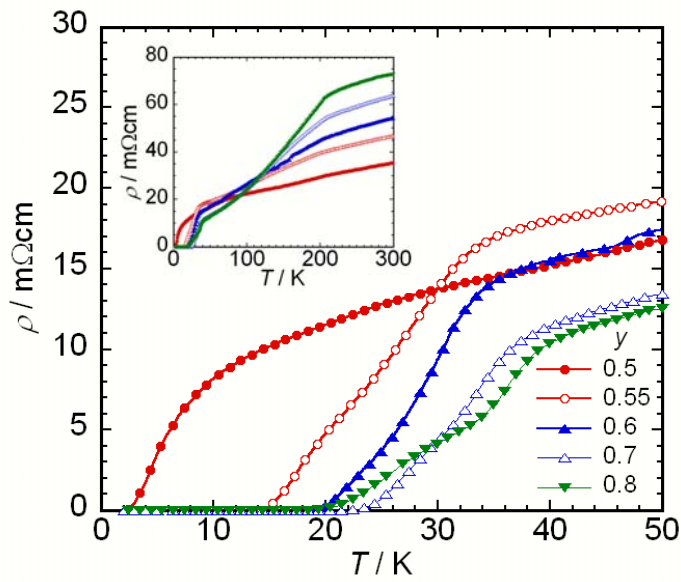


Figure 10

